Optimization of Carrier Multiplication for More Effcient Solar Cells: The Case of Sn Quantum Dots

Guy Allan and Christophe Delerue*

IEMN, Department ISEN, 41 boulevard Vauban, 59046 Lille Cedex, France

ABSTRACT We present calculations of impact ionization rates, carrier multiplication yields, and solar-power conversion efficiencies in solar cells based on quantum dots (QDs) of a semimetal, α-Sn. Using these results and previous ones on PbSe and PbS QDs, we discuss a strategy to select QDs with the highest carrier multiplication rate for more efficient solar cells. We suggest using QDs of materials with a close to zero band gap and a high multiplicity of the bands in order to favor the relaxation of photoexcited carriers by impact ionization. Even in that case, the improvement of the maximum solar-power conversion efficiency appears to be a challenging task.

KEYWORDS: quantum dot · carrier multiplication · Sn · nanocrystal · semiconductor · photovoltaics · solar cell

Carrier multiplication (CM) is a process in which more than one electron–hole pair is created as the result of the absorption of a single photon. CM has recently received considerable attention both experimentally[1−9] and theoretically[10−22] because it has the potential to improve the performance of solar cells.[23] The main origin of CM is the relaxation of photoexcited carriers by impact ionization[24] (Figure 1) which, above a certain energy threshold, becomes more efficient than the intraband relaxation by emission of phonons. In bulk Si, CM cannot be useful for solar-energy conversion because of its high threshold in photon energy (3.8 eV[25]). Therefore, a lot of efforts are devoted to find materials with more efficient CM for photons in the solar spectrum.

With this aim, it was proposed[10] to use semiconductor quantum dots (QDs) because the strong confinement breaks the momentum conservation rules which could enhance the impact ionization rate. This proposition seemed to be supported by early experiments on CM in QDs,[1−3] but unfortunately, all of the recent works have reported much less efficient CM,[4−8] even less than in the parent bulk when compared to an absolute photon energy basis.[9,21] This lower efficiency is, in fact, in agreement with our previous calculations of the impact ionization lifetimes, showing that momentum conservation is not a limiting factor at high excess energy of photoexcited carriers even in the bulk.[12] Therefore, the main role of quantum confinement is to shift the band gap to higher energy.[19,21] These arguments have been recently summarized by Nair *et al.*[21] in a critical analysis of the works on CM in QDs, but it is fair to mention that different opinions have been published.[7,8,26] The magnitude of the CM yields and the comparison between bulk materials and QDs remain sources of controversy in particular.[7−9,19,21,26]

Thus a new strategy is needed to select or design materials with the highest CM efficiency for solar-energy conversion purpose. As discussed in ref 21, the main challenge is to choose the best parent bulk material. In this article, we propose to start with a bulk material which has a very small band gap—or even a zero band gap—and a high density of states near the band edges. The quantum confinement is mainly used to tune the gap and thus the CM threshold with respect to the solar spectrum.[21] Calculations of the CM efficiency in α-Sn QDs are presented to support this proposition.

QDs with the Highest CM Efficiency. The CM efficiency is high when hot carriers decay to lower energy more favorably by impact ionization than by emission of phonons.[12,15] Therefore, our strategy can be understood from Figure 2, which shows the typical behavior of the mean impact ionization lifetime as a function of the energy of the photoexcited carriers, as deduced from our previous works[12,15] on different types of semiconductors. The strong dependence of the lifetime with energy is directly connected to the variation of the density of final states in the impact ionization process[12,13,17] since the average matrix element of the Coulomb interaction between the initial

* Address correspondence to christophe.delerue@isen.fr.

Received for review June 14, 2011 and accepted August 13, 2011.

Published online August 14, 2011
10.1021/nn202180u

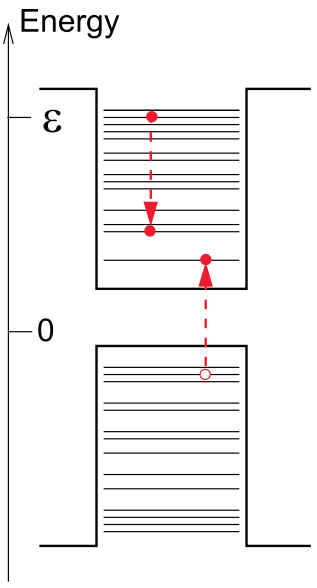

Figure 1. Schematics of the impact ionization process: a hot electron (energy $\varepsilon > 0$) decays to a lower energy state and excites an extra electron–hole pair. The process for the excited hole ($\varepsilon < 0$) is symmetric.

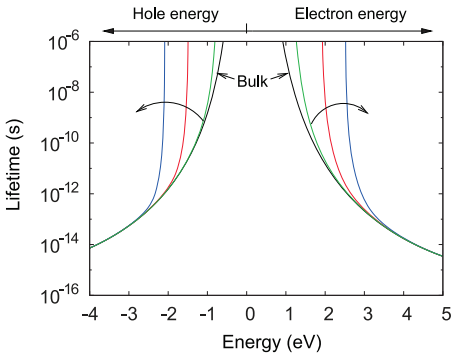

Figure 2. Typical behavior of the impact ionization lifetime *versus* the energy ε of the excited carrier. The evolution from the bulk semiconductor to QDs of decreasing size is indicated by the arrows. The time and energy scales are derived for the case of PbS,[12] but the rapid variations of the lifetime[12,15,17] have been smoothed out.

and final states can be considered as constant on this scale.[12] At a given energy, the lifetime is, on average, longer in QDs than in bulk due to a reduced density of final states, which implies that the impact ionization lifetime in QDs is always bounded by its bulk value. We conclude that the highest CM yield in QDs will be obtained by shifting the curves for the bulk in Figure 2 horizontally to lower carrier energy ($|\varepsilon| \rightarrow 0$) and vertically to smaller lifetime. The horizontal shift can be obtained using a small band gap material. The vertical shift, which can depend on energy, can be achieved by increasing the density of final states for impact ionization (*i.e.*, the number of combinations of three-particle states with the same total energy as shown in Figure 1), using a material with a high degeneracy of the band edges, for example.

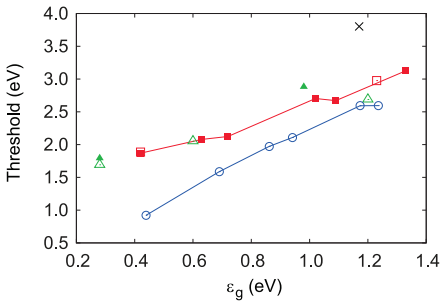

Figure 3. CM energy threshold plotted *versus* the gap energy ε_g for α-Sn (blue; open circles, present theory), PbS (red; filled squares, experiments;[9,27] open squares, theory[9,19]), PbSe (green; open triangles, theory;[19] filled triangles, experiments[28]), and bulk Si[25] (×).

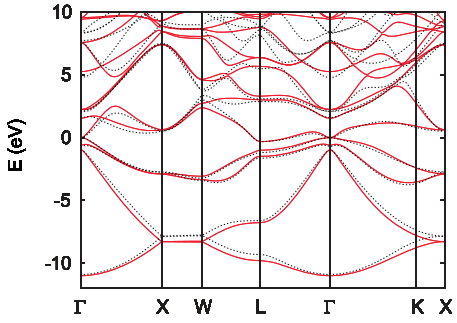

Figure 4. Band structure of α-Sn (solid red curves, *ab initio* calculations; dashed black curves, tight-binding calculations). The zero of energy corresponds to the Fermi level.

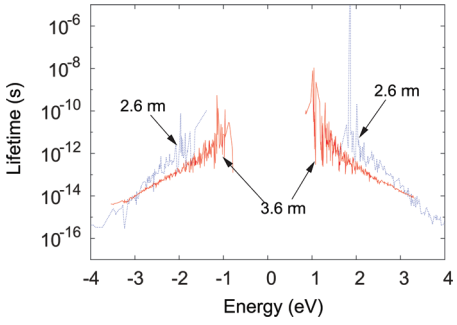

Figure 5. Impact ionization lifetime *versus* the energy ε of the excited carrier in α-Sn nanocrystals (red curve, diameter = 3.6 nm; blue curve, 2.6 nm). The zero energy corresponds to the bulk Fermi level.

This proposition is already in agreement with recent experimental and theoretical studies on PbSe and PbS showing that CM is more efficient in PbSe and PbS QDs than in bulk Si.[7–9,19,27,28] This is clearly visible in Figure 3, where we plot the evolution of the CM threshold with respect to the energy gap for different types of materials. Both theory and experiments show that the CM threshold for PbSe and PbS is much smaller than for bulk Si, even at the same energy gap. We argue that the superiority of PbSe and PbS compared to Si is due to their relatively small band gap (0.28 and 0.42 eV,

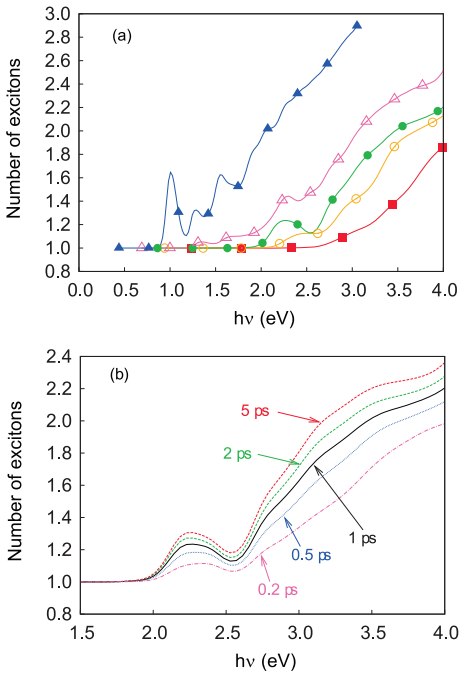

Figure 6. Number of excitons generated by impact ionization after the absorption of a photon of energy $h\nu$. (a) Results obtained with τ_{ph} = 1 ps for various QD sizes (filled blue triangles, ε_g = 0.44 eV; open magenta triangles, ε_g = 0.69 eV; filled green circles, ε_g = 0.86 eV; open orange circles, ε_g = 0.94 eV; red squares, ε_g = 1.24 eV). (b) Results obtained for ε_g = 0.86 eV and various values of τ_{ph}.

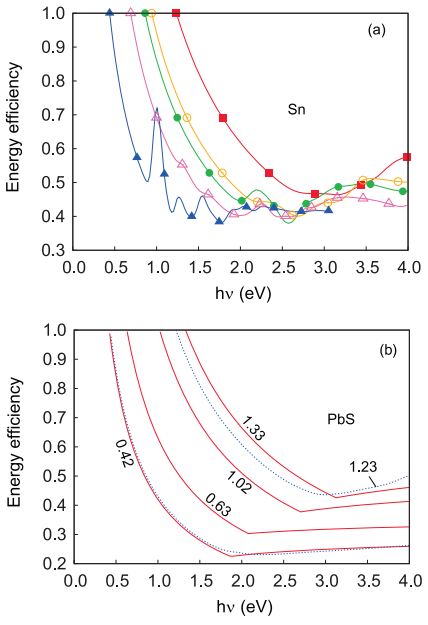

Figure 7. Energy efficiency *versus* photon energy. (a) Calculations for α-Sn QDs (filled blue triangles, ε_g = 0.44 eV; open magenta triangles, ε_g = 0.69 eV; filled green circles, ε_g = 0.86 eV; open orange circles, ε_g = 0.94 eV; red squares, ε_g = 1.24 eV). (b) Same for PbS QDs and bulk: derived from the experimental CM yields[9,27] (solid red lines); our calculations[9] (dotted blue lines). The value of ε_g in eV is indicated for each curve (0.42 eV for bulk PbS).

respectively) and the 8-fold degeneracy of their band edges at the L point of the Brillouin zone.

Impact Ionization in α-Sn QDs. If this strategy is correct, we anticipate that a smaller CM threshold could be obtained using materials with a smaller band gap than PbSe and PbS. In the following, we discuss the extreme case of α-Sn, a semimetal, whose band structure is shown in Figure 4. We consider α-Sn QDs in which a gap opens due to the quantum confinement.[29,30] We have chosen α-Sn as a test case because of its zero band gap, its high density of states near the Fermi level (see below), its very low toxicity, and the reported synthesis of QDs.[31−33] We compute the electronic structure of α-Sn QDs in tight-binding, and we calculate the impact ionization lifetime of photoexcited electrons and holes.

The impact ionization lifetime is plotted in Figure 5 as function of the energy ε for two QD sizes. It is smaller than 1 ps in a wide range of energy, and for the larger size (3.6 nm), it remains remarkably small even at low kinetic energy ($|\varepsilon| < 2$ eV), which is a direct consequence of the zero band gap of α-Sn (the "horizontal shift" discussed above).

CM in α-Sn QDs. Starting from these results, we simulate the CM process including the following steps:[12] (1) the optical absorption that determines the distribution of energies of the electron and the hole; (2) the relaxation either by impact ionization or by emission of phonons. We consider all possible initial energies of photogenerated carriers and all possible impact ionization relaxation channels including those leading to multiexciton generation. The methodology is described in ref 12. We assume that the lifetime for the intraband relaxation is a constant τ_{ph} independent of the energy.[12,15] For the sake of comparison, unless otherwise stated, the theoretical results presented here have been obtained with τ_{ph} = 1 ps. Values in this range have been reported experimentally[34−37] and have been typically used for simulations on PbSe, PbS, and Si.[9,12,19,22]

Figure 6a shows the CM yield (number of excitons per photon) in α-Sn QDs as function of the photon energy $h\nu$ for different values of ε_g between 0.44 and 1.24 eV. The evolution of the CM yield with τ_{ph} is presented in Figure 6b for QDs with ε_g = 0.86 eV. In contrast to PbSe, PbS,[12] Si, and InAs QDs,[15] the CM yield presents sharp peaks due to efficient optical transitions between electron/hole states characterized by high impact ionization rates. The CM thresholds deduced from Figure 6a are reported in Figure 3. For ε_g = 1.24 eV, the CM threshold is ≈1.2 eV smaller than for bulk Si and is even slightly smaller than for PbSe and PbS QDs with similar gap. Remarkably, when ε_g decreases, the CM threshold of α-Sn QDs continuously decreases while it clearly saturates above 1.8 eV for PbSe and PbS. The predicted threshold for α-Sn QDs varies ~2.15 × ε_g, close to its ideal limit of 2 × ε_g. This result demonstrates the benefit of small (even zero) band gap materials to obtain QDs with small CM threshold. The high density

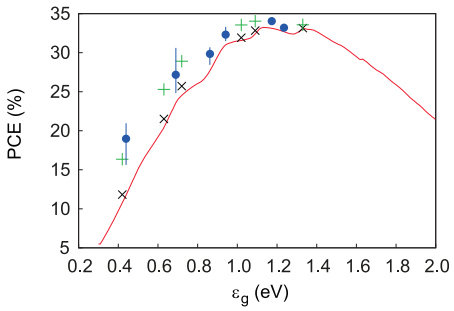

Figure 8. Calculated maximum solar-power conversion efficiency (PCE) for a single junction QD-based cell at normal incidence under AM1.5 illumination as a function of the energy gap: no CM (solid curve, red); PbS[9,27] (×, black); α-Sn (blue dots); PbS but with a threshold at 2 × ε_g (+, green). The blue vertical bars indicate the variation of the PCE for α-Sn when τ_{ph} varies from 0.1 to 10 ps (the bar is hidden by the dot symbol for the largest gaps).

of states near the Fermi level in bulk α-Sn induced by the presence of relatively flat bands (see the dispersion along $L-\Gamma-X$ in Figure 4) also contributes to obtaining a small CM threshold.

Energy Efficiency. The absence of band gap in α-Sn also has a strong influence on the energy efficiency. This quantity defined in ref 19 as the ratio between the total excitonic energy (number of excitons × ε_g) and $h\nu$ gives the relative amount of energy transformed into excitons instead of heat after relaxation of the carriers. Figure 7a shows that the energy efficiency always remains above 38% for α-Sn QDs, while for PbS (Figure 7b) and PbSe (Figure 4 of ref 19) QDs, it decreases to ∼25% for a small gap. This behavior is a direct consequence of the lower CM thresholds obtained for α-Sn QDs.

Power Conversion Efficiency. In order to evaluate the importance of CM for solar cells, we have calculated the power conversion efficiency (PCE) of a single junction cell under AM1.5 illumination using the detailed balance model.[38] The PCE for α-Sn and PbS QDs is shown in Figure 8. For α-Sn, we present the PCE obtained with τ_{ph} = 1 ps and its dispersion when τ_{ph} varies from 0.1 to 10 ps. In the case of PbS, the PCE is derived from the CM yields measured in ref 27. Compared to a solar cell without CM (red curve shown as a reference), the gain brought by the CM in PbS QDs is rather modest, whatever ε_g. Similar conclusion was obtained for PbSe QDs.[19] The reasons for the small contribution of the CM to the PCE in PbS and PbSe are given in Figure 3: (1) at $\varepsilon_g \approx 1$ eV, close to the maximum of the PCE curve, the CM threshold is too high in energy; and (2) for lower values of ε_g, the CM threshold saturates and does not follow the variations of ε_g. The role of the CM threshold is further demonstrated by the calculation of the PCE of PbS QDs, again using the CM yields measured in ref 27, but assuming an ideal CM threshold at 2 × ε_g. In that case, Figure 8 shows a significant enhancement of the PCE in a wide range of ε_g.

TABLE 1. Tight-Binding Parameters (Notations of Slater and Koster[40]) for α-Sn in an Orthogonal $sp^3d^5s^*$ Model (Δ Is the Spin−Orbit Coupling; Lattice Parameter = 6.47 Å)

parameters for Sn (eV)					
E_s	−5.32567	E_p	2.52194	E_d	12.06317
E_{s^*}	8.80303	Δ	0.25000		
$V_{ss\sigma}$	−1.26716	$V_{sp\sigma}$	1.79243	$V_{sd\sigma}$	−2.06445
$V_{ss^*\sigma}$	0.62601	$V_{s^*p\sigma}$	0.62509	$V_{s^*d\sigma}$	0.73680
$V_{pp\sigma}$	2.75609	$V_{pp\pi}$	−1.11032	$V_{pd\sigma}$	−1.27510
$V_{pd\pi}$	1.35105	$V_{pd\sigma}$	−2.33598	$V_{dd\pi}$	2.53095
$V_{dd\delta}$	−1.85318	$V_{s^*s^*\sigma}$	−0.93471		
parameters for Sn−H (eV)					
E_H	0.56000	$V_{ss\sigma}$	−5.15100	$V_{sp\sigma}$	5.27000

TABLE 2. Band Gap of α-Sn QDs *versus* Size

diameter (nm)	number of Sn atoms	band gap (eV)
2.31	191	1.24
2.49	239	1.17
2.61	275	0.94
2.77	329	0.86
2.91	381	0.69
3.57	705	0.44

In contrast to PbSe and PbS, we predict for α-Sn QDs an important contribution of the CM to the PCE especially for $\varepsilon_g \leq 0.9$ eV (Figure 8) because the CM threshold does not saturate but follows ε_g when it decreases (Figure 3). However, even in this favorable situation, the gain in PCE is only of 1.8% near the maximum ($\varepsilon_g \approx 1.1$ eV). It is clearly in this region that the improvement of the PCE is the most difficult to realize. It was shown[14,21] that a gain of ∼5% could be obtained near $\varepsilon_g \approx 1.1$ eV but only in an almost ideal situation characterized by a CM threshold at 2 × ε_g and a CM yield profile with a high slope. If, in α-Sn QDs, the predicted threshold is low, the slope of the CM yield after the threshold (Figure 6) is smaller than in PbSe (Figure 2 of ref 19) or PbS[27] due to a smaller density of final states for impact ionization. Thus there is still room for improvement if we can find a material with higher multiplicity of bands.

CONCLUSION

Our calculations on α-Sn QDs and the present knowledge on PbS and PbSe QDs suggest that the best candidate for QDs with a high CM efficiency should be found among materials with a close to zero band gap and a high multiplicity of the bands such that the density of final states for impact ionization is enhanced. The main role of the quantum confinement is to open a gap fitting with the solar spectrum. We predict that the PCE of solar cells based on α-Sn QDs should be substantially improved by the CM at low energy gap (<0.9 eV), but the

enhancement of the PCE at the maximum ($\varepsilon_g \approx 1.1$ eV) remains challenging as it requires fine-tuning of the CM yield profile. In this regard, Sb or Bi[39] could be considered as promising materials, but others, like InSb suggested in ref 21, could fulfill the same requirements.

METHODS

Electronic Structure of α-Sn QDs. We calculate the electronic structure of the QDs in tight-binding using a $sp^3d^5s^*$ basis and interactions restricted to first nearest neighbors. The parameters (Table 1) are obtained by fitting a reference bulk band structure (Figure 4) calculated *ab initio* in the local density approximation using the ABINIT code[41] and the Hartwigsen–Goedecker–Hutter pseudopotential.[42] The tight-binding parameters are transferred without change from bulk to QDs. The surface of QDs is passivated with pseudo-hydrogen atoms. The band gap *versus* size of the QDs considered in this work is given in Table 2.

Calculation of the Impact Ionization Lifetime. The impact ionization lifetime in α-Sn QDs is obtained using basically the same method as in our previous works on PbSe, PbS, InAs, and Si QDs[12,15] except that, in the matrix elements of the screened Coulomb (electron–electron) interaction, we consider the full frequency dependence[43] because the opening of the gap (from zero) influences the screening properties. The frequency-dependent screened Coulomb interaction in QDs is calculated in the random-phase approximation in tight-binding as described in ref 44.

Acknowledgment. This work was supported by the EU Seventh Framework Program (EU-FP7 ITN Herodot) and by the French Ministry of Defense under Grant No. 2008.34.0031.

REFERENCES AND NOTES

1. Schaller, R. D.; Klimov, V. I. High Effciency Carrier Multiplication in PbSe Nanocrystals: Implications for Solar Energy Conversion. *Phys. Rev. Lett.* **2004**, *92*, 186601-1/4.
2. Ellingson, R.; Beard, M.; Johnson, J.; Yu, P.; Micic, O.; Nozik, A.; Shabaev, A.; Efros, A. Highly Effcient Multiple Exciton Generation in Colloidal PbSe and PbS Quantum Dots. *Nano Lett.* **2005**, *5*, 865–871.
3. Pijpers, J. J. H.; Hendry, E.; Milder, M. T. W.; Fanciulli, R.; Savolainen, J.; Herek, J. L.; Vanmaekelbergh, D.; Ruhman, S.; Mocatta, D.; Oron, D.; *et al.* Carrier Multiplication and Its Reduction by Photodoping in Colloidal InAs Quantum Dots. *J. Phys. Chem. C* **2007**, *111*, 4146–4152.
4. Pijpers, J. J. H.; Hendry, E.; Milder, M. T. W.; Fanciulli, R.; Savolainen, J.; Herek, J. L.; Vanmaekelbergh, D.; Ruhman, S.; Mocatta, D.; Oron, D.; *et al.* Carrier Multiplication and Its Reduction by Photodoping in Colloidal InAs Quantum Dots (erratum). *J. Phys. Chem. C* **2008**, *112*, 4783–4784.
5. Trinh, M. T.; Houtepen, A. J.; Schins, J. M.; Hanrath, T.; Piris, J.; Knulst, W.; Goossens, A. P. L. M.; Siebbeles, L. D. A. In Spite of Recent Doubts Carrier Multiplication Does Occur in PbSe Nanocrystals. *Nano Lett.* **2008**, *8*, 1713–1718.
6. Nair, G.; Geyer, S. M.; Chang, L.-Y.; Bawendi, M. G. Carrier Multiplication Yields in PbS and PbSe Nanocrystals Measured by Transient Photoluminescence. *Phys. Rev. B* **2008**, *78*, 125325–1/10.
7. McGuire, J. A.; Joo, J.; Pietryga, J. M.; Schaller, R. D.; Klimov, V. I. New Aspects of Carrier Multiplication in Semiconductor Nanocrystals. *Acc. Chem. Res.* **2008**, *41*, 1810–1819.
8. McGuire, J. A.; Sykora, M.; Joo, J.; Pietryga, J. M.; Klimov, V. I. Apparent *versus* True Carrier Multiplication Yields in Semiconductor Nanocrystals. *Nano Lett.* **2010**, *10*, 2049–2057.
9. Pijpers, J. J. H.; Ulbricht, R.; Tielrooij, K. J.; Osherov, A.; Golan, Y.; Delerue, C.; Allan, G.; Bonn, M. Assessment of Carrier-Multiplication Effciency in Bulk PbSe and PbS. *Nat. Phys.* **2009**, *5*, 811–814.
10. Nozik, A. Spectroscopy and Hot Electron Relaxation Dynamics in Semiconductor Quantum Wells and Quantum Dots. *Annu. Rev. Phys. Chem.* **2001**, *52*, 193–231.
11. Schaller, R.; Agranovich, V.; Klimov, V. High-Effciency Carrier Multiplication through Direct Photogeneration of Multi-excitons *via* Virtual Single-Exciton States. *Nat. Phys.* **2005**, *1*, 189–194.
12. Allan, G.; Delerue, C. Role of Impact Ionization in Multiple Exciton Generation in PbSe Nanocrystals. *Phys. Rev. B* **2006**, *73*, 205423-1/5.
13. Franceschetti, A.; An, J. M.; Zunger, A. Impact Ionization Can Explain Carrier Multiplication in PbSe Quantum Dots. *Nano Lett.* **2006**, *6*, 2191–2195.
14. Hanna, M. C.; Nozik, A. J. Solar Conversion Effciency of Photovoltaic and Photoelectrolysis Cells with Carrier Multiplication Absorbers. *J. Appl. Phys.* **2006**, *100*, 074510-1/8.
15. Allan, G.; Delerue, C. Influence of Electronic Structure and Multiexciton Spectral Density on Multiple-Exciton Generation in Semiconductor Nanocrystals: Tight-Binding Calculations. *Phys. Rev. B* **2008**, *77*, 125340-1/10.
16. Luo, J. W.; Franceschetti, A.; Zunger, A. Carrier Multiplication in Semiconductor Nanocrystals: Theoretical Screening of Candidate Materials Based on Band-Structure Effects. *Nano Lett.* **2008**, *8*, 3174–3181.
17. Rabani, E.; Baer, R. Distribution of Multiexciton Generation Rates in CdSe and InAs Nanocrystals. *Nano Lett.* **2008**, *8*, 4488–4492.
18. Sevik, C.; Bulutay, C. Auger Recombination and Carrier Multiplication in Embedded Silicon and Germanium Nanocrystals. *Phys. Rev. B* **2008**, *77*, 125414-1/4.
19. Delerue, C.; Allan, G.; Pijpers, J. J. H.; Bonn, M. Carrier Multiplication in Bulk and Nanocrystalline Semiconductors: Mechanism, Effciency, and Interest for Solar Cells. *Phys. Rev. B* **2010**, *81*, 125306-1/6.
20. Rabani, E.; Baer, R. Theory of Multiexciton Generation in Semiconductor Nanocrystals. *Chem. Phys. Lett.* **2010**, *496*, 227–235.
21. Nair, G.; Chang, L.-Y.; Geyer, S. M.; Bawendi, M. G. Perspective on the Prospects of a Carrier Multiplication Nanocrystal Solar Cell. *Nano Lett.* **2011**, *11*, 2145–2151.
22. Velizhanin, K. A.; Piryatinski, A. Numerical Study of Carrier Multiplication Pathways in Photoexcited Nanocrystal and Bulk Forms of PbSe. *Phys. Rev. Lett.* **2011**, *106*, 207401-1/4.
23. Werner, J. H.; Kolodinski, S.; Queisser, H. J. Novel Optimization Principles and Effciency Limits for Semiconductor Solar Cells. *Phys. Rev. Lett.* **1994**, *72*, 3851–3854.
24. Landsberg, P. T. *Recombination in Semiconductors*; Cambridge University Press: Cambridge, UK, 1991.
25. Wolf, M.; Brendel, R.; Werner, J. H.; Queisser, H. J. Solar Cell Effciency and Carrier Multiplication in $Si_{1-x}Ge_x$ Alloys. *J. Appl. Phys.* **1998**, *83*, 4213–4221.
26. Beard, M. C.; Midgett, A. G.; Hanna, M. C.; Luther, J. M.; Hughes, B. K.; Nozik, A. J. Comparing Multiple Exciton Generation in Quantum Dots to Impact Ionization in Bulk Semiconductors: Implications for Enhancement of Solar Energy Conversion. *Nano Lett.* **2010**, *10*, 3019–3027.
27. Nootz, G.; Padilha, L. A.; Levina, L.; Sukhovatkin, V.; Webster, S.; Brzozowski, L.; Sargent, E. H.; Hagan, D. J.; Van Stryland, E. W. Size Dependence of Carrier Dynamics and Carrier Multiplication in PbS Quantum Dots. *Phys. Rev. B* **2011**, *83*, 155302-1/7.
28. Trinh, M. T.; Polak, L.; Schins, J. M.; Houtepen, A. J.; Vaxenburg, R.; Maikov, G. I.; Grinbom, G.; Midgett, A. G.; Luther, J. M.; Beard, M. C.; *et al.* Anomalous Independence of Multiple Exciton Generation on Different Group IV–VI Quantum Dot Architectures. *Nano Lett.* **2011**, *11*, 1623–1629.

29. Pedersen, T. G.; Fisker, C.; Jensen, R. V. Tight-Binding Parameterization of α-Sn Quasiparticle Band Structure. *J. Phys. Chem. Solids* **2010**, *71*, 18–23.
30. Moontragoon, P.; Vukmirović, N.; Ikonić, Z.; Harrison, P. Electronic Structure and Optical Properties of Sn and SnGe Quantum Dots. *J. Appl. Phys.* **2008**, *103*, 103712-1/8.
31. Arslan, I.; Yates, T. J. V.; Browning, N. D.; Midgley, P. A. Embedded Nanostructures Revealed in Three Dimensions. *Science* **2005**, *309*, 2195–2198.
32. Karim, A.; Hansson, G.; Ni, W.-X.; Holtz, P.; Larsson, M.; Atwater, H. Photoluminescence Studies of Sn Quantum Dots in Si Grown by MBE. *Opt. Mater.* **2005**, *27*, 836–840 Si-based Photonics: Towards True Monolithic Integration—Proceedings of the European Materials Research Society, Symposium A1, European Materials Research Society 2004 Spring Meeting.
33. Lei, Y.; Mock, P.; Topuria, T.; Browning, N. D.; Ragan, R.; Min, K. S.; Atwater, H. A. Void-Mediated Formation of Sn Quantum Dots in a Si Matrix. *Appl. Phys. Lett.* **2003**, *82*, 4262–4264.
34. Wehrenberg, B. L.; Wang, C.; Guyot-Sionnest, P. Interband and Intraband Optical Studies of PbSe Colloidal Quantum Dots. *J. Phys. Chem. B* **2002**, *106*, 10634–10640.
35. Okuno, T.; Masumoto, Y.; Ikezawa, M.; Ogawa, T.; Lipovskii, A. Size-Dependent Picosecond Energy Relaxation in PbSe Quantum Dots. *Appl. Phys. Lett.* **2000**, *77*, 504–506.
36. Harbold, J. M.; Du, H.; Krauss, T. D.; Cho, K.-S.; Murray, C. B.; Wise, F. W. Time-Resolved Intraband Relaxation of Strongly Confined Electrons and Holes in Colloidal PbSe Nanocrystals. *Phys. Rev. B* **2005**, *72*, 195312-1/6.
37. Bonati, C.; Cannizzo, A.; Tonti, D.; Tortschanoff, A.; van Mourik, F.; Chergui, M. Subpicosecond Near-Infrared Fluorescence Upconversion Study of Relaxation Processes in PbSe Quantum Dots. *Phys. Rev. B* **2007**, *76*, 033304-1/4.
38. Brendel, R.; Werner, J. H.; Queisser, H. J. Thermodynamic Efficiency Limits for Semiconductor Solar Cells with Carrier Multiplication. *Sol. Energy Mater. Sol. Cells* **1996**, *41*−*42*, 419–425.
39. Gonze, X.; Michenaud, J.-P.; Vigneron, J.-P. First-Principles Study of As, Sb, and Bi Electronic Properties. *Phys. Rev. B* **1990**, *41*, 11827–11836.
40. Slater, J. C.; Koster, G. F. Simplified LCAO Method for the Periodic Potential Problem. *Phys. Rev.* **1954**, *94*, 1498–1524.
41. Gonze, X.; Amadon, B.; Anglade, P.-M.; Beuken, J.-M.; Bottin, F.; Boulanger, P.; Bruneval, F.; Caliste, D.; Caracas, R.; Côté, M.; *et al.* ABINIT: First-Principles Approach to Material and Nanosystem Properties. *Comput. Phys. Commun.* **2009**, *180*, 2582–2615.
42. Hartwigsen, C.; Goedecker, S.; Hutter, J. Relativistic Separable Dual-Space Gaussian Pseudopotentials from H to Rn. *Phys. Rev. B* **1998**, *58*, 3641–3662.
43. Kane, E. O. Electron Scattering by Pair Production in Silicon. *Phys. Rev.* **1967**, *159*, 624–631.
44. Delerue, C.; Lannoo, M.; Allan, G. Calculations of the Electron-Energy-Loss Spectra of Silicon Nanostructures and Porous Silicon. *Phys. Rev. B* **1997**, *56*, 15306–15313.